ADVANCED FUNCTIONAL MATERIALS
www.afm-journal.de

Quantitative Recovery of Magnetic Nanoparticles from Flowing Blood: Trace Analysis and the Role of Magnetization

*Christoph M. Schumacher, Inge K. Herrmann, Stephanie B. Bubenhofer, Sabrina Gschwind, Ann-Marie Hirt, Beatrice Beck-Schimmer, Detlef Günther, and Wendelin J. Stark**

Magnetic nanomaterials find increasing application as separation agents to rapidly isolate target compounds from complex biological media (i.e., blood purification). The responsiveness of the used materials to external magnetic fields (i.e., their saturation magnetization) is one of the most critical parameters for a fast and thorough separation. In the present study, magnetite (Fe_3O_4) and non-oxidic cementite (Fe_3C) based carbon-coated nanomagnets are characterized in detail and compared regarding their separation behavior from human whole blood. A quantification approach for iron-based nanomaterials in biological samples with strong matrix effects (here, salts in blood) based on platinum spiking is shown. Both materials are functionalized with polyethyleneglycol (PEG) to improve cytocompatibility (confirmed by cell toxicity tests) and dispersability. The separation performance is tested in two setups, namely under stationary and different flow-conditions using fresh human blood. The results reveal a superior separation behavior of the cementite based nanomagnets and strongly suggest the use of nanomaterials with high saturation magnetizations for magnetic retention under common blood flow conditions such as in veins.

1. Introduction

Magnetic nanomaterials allow fascinating perspectives for biomedical applications.[1] Particularly in targeted drug delivery,[2] as contrast agents,[3] magnetic hyperthermia in cancer-treatment,[4] magnetic labeling[5] and blood or tissue purification.[6–8] The ease to provoke a physical movement of a desired constituent through applications of an external magnetic field in a tissue pervading manner is most attractive. Movement is essentially controlled by the magnetic characteristics and volume of a particle next to the magnetic field's properties (strength and gradient). Decreasing the particle size in favor of a high-surface to volume ratio and mobility weakens the magnetic responsiveness.[9] Consequently, targeting of deep tissue sites and re-collection of magnetic particles under flow conditions (magnetic dialysis) requires particles with high magnetic moments. The size constraints imply that efficient magnetic targeting solely relies on the magnetic properties of the core material. Among the ferromagnetic elements iron, cobalt and nickel, the last two have been associated with adverse side effects at relatively low plasma concentrations (e.g., metal-on-metal hip implants).[10] Physiologically well-accepted iron in the form of polymer or silica coated magnetite exhibits a pronounced saturation magnetization (typically <60 emu g^{-1}) and can easily be obtained as nano-sized and even superparamagnetic (i.e., no remaining magnetic moment without external field) particles by wet phase chemistry.[11] Carbon-encapsulated non-oxidic cementite (Fe_3C) nanoparticles with a chemically stable C-coating have recently become available through reducing flame spray synthesis.[12] Cementite has an even higher saturation magnetization (up to 140 emu g^{-1}) than magnetite. The well-structured few-layer carbon surface coating furthermore offers a platform for stable covalent chemical functionalizations.[13]

Here, we report the synthesis and detailed physical and magnetic characterization of both magnetite and cementite particles with platinum doping (0.1 wt%) to establish an analytical tool for quantification of magnetic particles in biological samples with strong matrix effects (iron, salts in blood or tissue). A low detection limit for the nanoparticles was achieved through quantitative platinum analysis by inductively coupled plasma mass spectrometry. Platinum is chemically inert, not abundant in living organisms and therefore well-suited for analytical

C. M. Schumacher, S. B. Bubenhofer, Prof. W. J. Stark
ETH Zurich, Institute for Chemical and Bioengineering
Wolfgang-Pauli-Strasse 10, CH-8093
Zurich Switzerland
E-mail: wendelin.stark@chem.ethz.ch
Dr. I. K. Herrmann, Prof. B. Beck-Schimmer
University Hospital Zurich
Institute of Anesthesiology
Rämistrasse 100, CH-8091 Zurich, Switzerland
S. Gschwind, Prof. D. Günther
ETH Zurich, Laboratory of Inorganic Chemistry
Wolfgang-Pauli-Strasse 10, CH-8093 Zurich, Switzerland
Prof. A.-M. Hirt
ETH Zurich, Institute of Geophysics
Sonneggstrasse 5, CH-8092 Zurich, Switzerland

DOI: 10.1002/adfm.201300696

purposes. Both materials were functionalized with polyethylene glycol (PEG) surface groups to enhance dispersibility.[14–16] Recently, the detoxification of contaminated human whole blood using cementite nanoparticles was reported.[7] Due to its viscosity, the thorough separation of a magnetic nanomaterial from blood within a reasonable time-frame is challenging. We compared a stationary separation (no liquid movement) of the magnetic particles from fresh human whole blood. Secondly, we analyzed the effectiveness of separation under continuous blood flow representing in vivo conditions in small (venules, tissue level) or even larger human veins (e.g., vena cubitalis, brachialis). Non-oxidic magnetic cementite nanoparticles could be quantitatively recollected even from flowing blood while less magnetic oxide-based nanoparticles stayed in the blood stream. The capability to reliably inject and remove a magnetic particle from flowing blood offers attractive perspectives for the development of novel treatment concepts such as in vivo extraction of toxins or infectious agents.

2. Experimental Section

2.1. Nanomaterial Synthesis

Precursor Synthesis: Platinum acetylacetonate (0.435 g, ≥ 98%, ABCR-Chemicals) was dissolved in a mixture of 2-ethylhexanoic acid (≥ 99%, Sigma-Aldrich) and tetrahydrofuran (THF) (≥ 99%, Fisher Scientific) (60 mL, weight:weight ratio 1:1) to give a brownish precursor solution.

An aqueous 25% NH_3 solution (688 g, Merck) was added stepwise to 2-ethylhexanoic acid (1442 g, technical grade, Soctech) using external cooling by an ice-water bath. Hereafter, $FeNO_3{\cdot}9H_2O$ (1820 g, ≥ 98%, ABCR-Chemicals) was added successively under vigorous stirring. A brown, very viscous mixture resulted. Pentane (≥ 98%, Sigma-Aldrich) was added at discretion to obtain a reasonable viscosity to separate and reject the aqueous phase. Thereafter, the organic phase was dried using anhydrous $MgSO_4$ (≥ 99.5%, Sigma-Aldrich) and filtrated. The pentane was removed by distillation, resulting in a highly viscous brown liquid.

The metal content of the platinum precursor was calculated from the initial weights of all used substances (0.4 wt% Pt). The iron-content of the Fe-precursor was determined by adding small amounts of precursor into Erlenmeyer-flasks and burning of the organic contents by heating to 600 °C for 2 h. Hereafter, the composition of the residues was determined using X-ray diffraction (XRD). By measuring the mass of the residues (pure Fe_2O_3) and knowing the initial amounts of precursor which was burnt, the metal content was calculated (11.4 wt% Fe).

Platinum Spiked Magnetite Nanoparticles: The platinum and the iron precursor were mixed at a ratio to target 0.1 wt% platinum in magnetite (Fe_3O_4). This mixture was further diluted with THF (weight-ratio precursor:THF 2:1) and then used in a partially reducing flame-spray synthesis unit as previously described.[17] The oxygen content of the environment during the production was kept at a concentration of around 200–500 ppm (confirmed by online mass-spectroscopy). The resulting black powder was characterized by XRD, element microanalysis, magnetic hysteresis and first-order reversal curve (FORC) analysis.

Carbon-Coated Platinum Spiked Cementite Nanoparticles: The platinum and the iron precursor were mixed to target 0.1 wt% platinum in cementite (Fe_3C) and then diluted with THF (weight-ratio precursor:THF 2:1). Carbon-coated platinum-spiked cementite particles were produced in a reducing flame-spray synthesis unit with an entering acetylene stream above the flame.[12,13] The oxygen content in the atmosphere was kept below 40 ppm during the synthesis. The resulting platinum-spiked carbon-coated cementite particles were thoroughly washed in HCl (24%) for 1 week in total (acid exchange every day) to remove material which was improperly coated with carbon. By this procedure around 40 wt% of the material is lost, yielding a chemically very stable fraction of particles.[18] The resulting black powder was characterized by XRD, elemental microanalysis, hysteresis and FORC analysis.

2.2. Chemical Functionalization

PEG-Functionalization of Platinum Spiked Magnetite Nanoparticles: As-prepared platinum-spiked magnetite particles (100 mg), consecutively termed as Pt/Fe_3O_4, were added to DMF (50 mL, ≥ 99%, Sigma-Aldrich) and dispersed by ultrasonication. Thereafter, methoxy-polyethyleneglycol-nitrodopamine (10 mg, molecular weight 5000 Da, SuSoS Surface Technology) was added. The dispersion was stirred for 24 h at 50 °C following previously established protocols.[16] After this, the particles were separated magnetically, washed with dimethylformamide (DMF) (2x), H_2O (1x), 2-propanol (2x) and then dried under vacuum. The surface functionality was confirmed by diffuse reflectance infrared Fourier transform spectroscopy (DRIFTS) and element microanalysis. The functionalized particles are subsequently termed as PEG-Pt/Fe_3O_4.

PEG-Functionalization of Carbon-Coated Platinum Spiked Cementite Nanoparticles: Following pre-established protocols,[7] thiophenol groups were grafted covalently to the carbon-surface of as-prepared platinum-spiked carbon-coated cementite particles, consecutively termed as $Pt/C/Fe_3C$, using aqueous diazonium chemistry. The functional attachment was verified by DRIFTS and quantified by element microanalysis. $Pt/C/Fe_3C$ (500 mg) was dispersed in phosphate-buffered saline (PBS) solution (50 mL, pH 7.2, 10 mM EDTA) by ultrasonication. Methoxy-polyethyleneglycol-maleimide (100 mg, molecular weight 5000 Da, NanoCS) was dissolved in dimethylacetamide (25 mL, ≥ 99.5%, Acros).[19] Both solutions were mixed and then stirred for 6 h at room temperature. After this, the particles were washed with H_2O (3x), ethanol (3x), dried under vacuum and again characterized by DRIFTS and elemental microanalysis. The particles are subsequently termed as PEG-$Pt/C/Fe_3C$.

Stationary Magnetic Separation from Human Whole Blood: PEG-Pt/Fe_3O_4 (25 mg), respectively PEG-$Pt/C/Fe_3C$ particles (25 mg) were dispersed in PBS (5 mL, pH 7.4) by ultrasonication. Portions (200 µL) of these dispersions were added to citrated human whole blood samples (800 µL) in glass vials (diameter 28 mm) to achieve initial particle concentrations of 1 mg particles per mL of fresh human blood. Every donor had signed a written consent approved by the ethical commission of Zurich

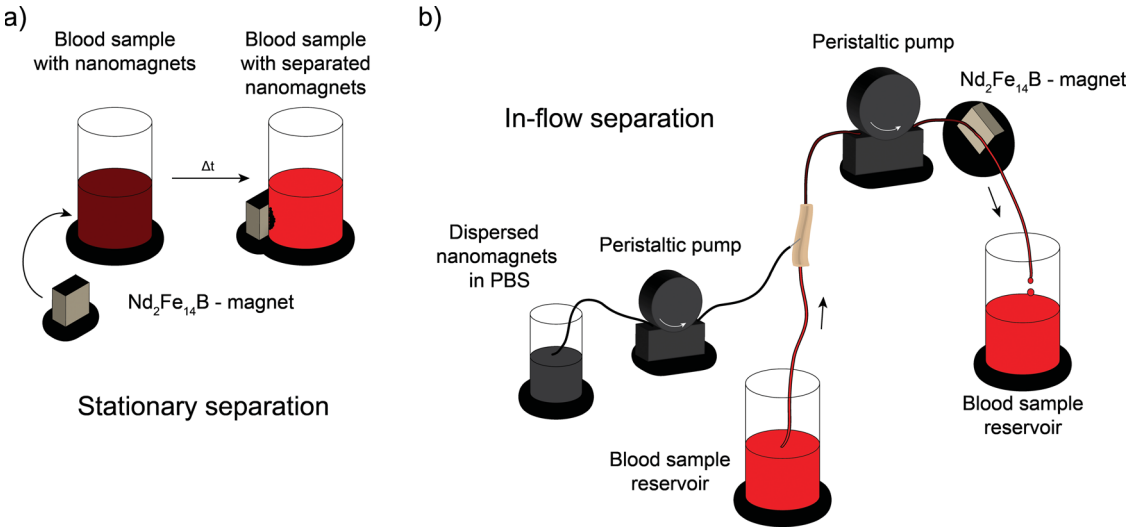

Figure 1. a) A stationary magnetic separation setup was used to monitor the performance to remove magnetic materials from human whole blood using an ultra-strong permanent magnet which was placed at the side of a glass vial for different times. b) Well-dispersed nanomagnets in PBS were pumped into a flowing blood-stream and were later removed with a strong magnet which was placed at the side-wall of the silicone tubing. The flow-rate of both the nanomagnet-dispersion and the blood stream can be adjusted and results in different separation performances.

(No. KEK-ZH 2012-0274) prior to the donation. In volunteers, after having obtained written informed consent, 5 tubes (4.5 mL, 0.129 M sodium citrate, Vacutainer) were withdrawn. After brief shaking an ultra-strong magnet ($Nd_2Fe_{14}B$ 12 × 12 × 12 mm, ≈0.5 Tesla) was placed near the samples for distinct times (10 s, 30 s, 1 min, 3 min, 30 min and 60 min) to separate the magnetic material as shown in **Figure 1**a. The particle content of the extracted blood samples was analyzed by the use of inductively coupled plasma mass spectrometry (ICP-MS).

In-Flow Magnetic Separation from Human Whole Blood: A setup, depicted in Figure 1b, was established to remove the different nanomaterials from flowing heparinized blood/particle-streams at a high and a low flow-rate (1 mL min^{-1} and 12.5 mL min^{-1}, respectively 2.4 mm s^{-1} and 30 mm s^{-1} average blood flow rate). Therefore, PEG-Pt/Fe_3O_4 (25 mg) or PEG-Pt/C/Fe_3C particles (25 mg) were dispersed in buffer (5 mL, PBS, pH 7.4) using 30 mL glass vials to give a particle concentration of 5 mg mL^{-1}. This dispersion was pumped into blood streams at rates of 0.2 mL min^{-1}, respectively 2.5 mL min^{-1}, using a peristaltic pump. The blood was pumped at 1 or 12.5 mL min^{-1} using a second peristaltic pump approved for hemodialysis. After this pump the nanomaterial was re-collected using an ultra-strong permanent magnet ($Nd_2Fe_{14}B$ 12 × 12 × 12 mm, ≈0.5 Tesla) which was placed at the side of the silicone-tube (3 mm inner diameter, 0.5 mm wall thickness).

2.3. Particle Quantification in Blood Samples

Blood samples (typical amount of 1 g) spiked with known amounts of particles as well as the extracted blood samples were given into poly(tetrafluoroethylene) digestion tubes. Then HNO_3 (65%), HCl (37%) and H_2O_2 (35%) at typical amounts of 1 g each were added. An additional rhodium spike of 0.25 mg kg^{-1} acted as a recovery-standard for the digestion. The samples were treated at 200 °C and 40 bar in a microwave based digestion system (ultaCLAVE II, Milestone Inc.). After this treatment the samples were diluted to 1:50 with respect to the initial blood sample amount using an acidic mixture containing HCl (1%, v/v) and HNO_3 (1%, v/v). Thereafter the samples were further diluted 1:20 and spiked with iridium as an internal standard (2.5 µg kg^{-1}). Suitable salt and acid concentrations for a measurement by ICP-MS were achieved using this treatment. The corresponding calibration standards containing Rh (blank-7 µg kg^{-1}), Pt (blank-3.5 µg kg^{-1}) and Ir (2.5 µg g^{-1}) were prepared from blank blood samples to obtain the same blood matrix levels compared to the samples. Platinum concentrations and rhodium recoveries were quantified using a sector-field ICP-MS suitable for ultra-trace element analysis (Element 2, Thermo Fisher Scientific) by measuring the isotopes ^{103}Rh, ^{193}Ir, ^{194}Pt and ^{195}Pt.

2.4. Particle Degradation and Leaching

Due to their high specific surface area and depending on their chemical resistivity, material leaching into surrounding solutions is a frequently observed phenomenon for numerous nanomaterials. In order to test the leaching liability under physiological conditions, small amounts of both PEG functionalized particles (1 mg) were given into PBS (3 mL) and then stirred vigorously for 1 h. For a comparison under harsher, but not biologically relevant conditions, the same experiment was carried out in HCl (3 mL, 0.1 M). After the nanomaterials were withdrawn magnetically from the supernatant and a drop of concentrated HCl was added to the PBS samples, a small amount of potassium thiocyanate was added to form the orange iron-thiocyanate complex. Solutions with known iron concentrations acted as calibration standards for an iron concentration determination by UV-VIS spectroscopy at 467 nm. The strong color of the iron-thiocyanate complex allows a simple quantification

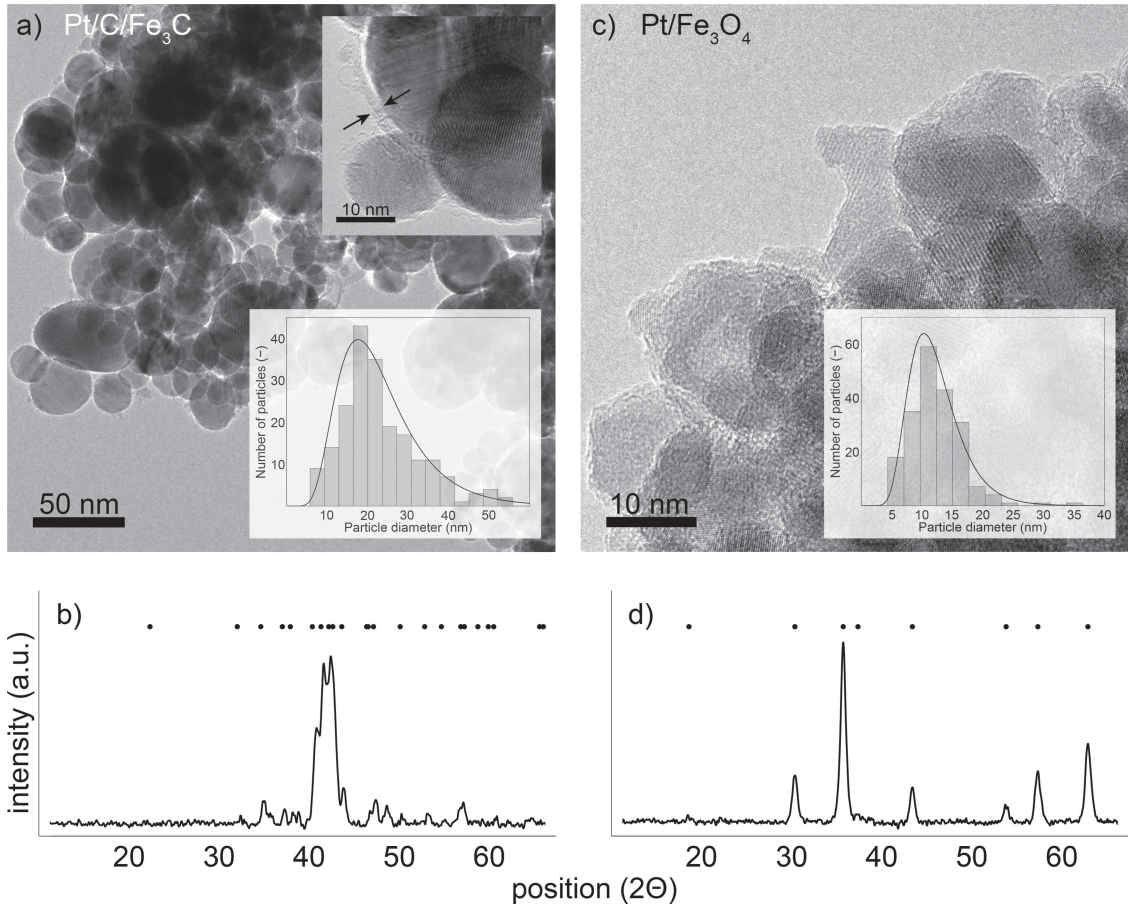

Figure 2. a) TEM showing spherical platinum-spiked cementite particles in the size-range of 10–50 nm. The insertion in the upper right depicts the multi-layer graphene-like stacked structure of the carbon-coating, which is responsible for an extraordinary chemical stability. c) Transmission electron micrograph of platinum-spiked magnetite particles in the size-range of 5–25 nm. b) The cementite and d) the magnetite structure were both confirmed by X-ray powder diffraction. No indications for a segregated platinum phase were found.

of iron (limit of detection ≈0.2 mg kg^{-1}). This allowed the calculation of the percentage of degraded particles.

2.5. Cell Compatibility Tests

Human microvascular endothelial cells (HMVEC, Lonza, Basel, Switzerland) were cultured as described elsewhere.[20] Cells were seeded in 96-well culture dishes (100 000 cells mL^{-1}, 0.1 mL per well). Both PEG-Pt/Fe_3O_4 and PEG-Pt/C/Fe_3C were predispersed in PBS. The cells were then incubated with magnetic nanoparticles dispersed in cell culture medium (10 and 100 mg kg^{-1}). Lipopolysaccharide (LPS from *Escherichia coli*, serotype 055:B5 (2 µg mL^{-1}, Sigma-Aldrich, Buchs, Switzerland) was used as positive control. After incubation for 20 h, supernatants were collected and centrifuged. For cytotoxicity assays, some wells were incubated with lysing solution (from the assay kit, Promega, Madison, WI, USA) for 1 h (100% lysis, maximum lactate dehydrogenase (LDH) release). Cytotoxicity was measured following the manufacturer's protocol and values were calculated relative to the positive control (100% lysis). ELISAs for human interleukin-6 were performed following the manufacturer's protocol (R&D Systems Europe Ltd, Abingdon, UK).

3. Results and Discussion

In a flame spray pyrolysis process under reducing atmosphere, iron-based magnetic nanoparticles with either magnetite (Fe_3O_4) or cementite (Fe_3C) cores were synthesized. As with growing applications of magnetic nanoparticles their detection in complex samples becomes increasingly important, the nanoparticles were spiked in situ with a tiny amount of platinum which serves as a tracer for particle detection in iron-rich biological sample matrices. The physicochemical characteristics of the nanoparticles including the shape, the size distribution, the magnetic properties and cytocompatibility were compared before the performance of the magnetic beads was assessed in a stationary and an in-flow magnetic separation process.

3.1. Material Characterization–Physicochemical Properties

The transmission electron microscopy (TEM) in **Figure 2**a shows spherical carbon-coated cementite nanoparticles with a size distribution between 10 and 50 nm. The carbon-coating appears as a few-layer graphene-like stacked structure, with

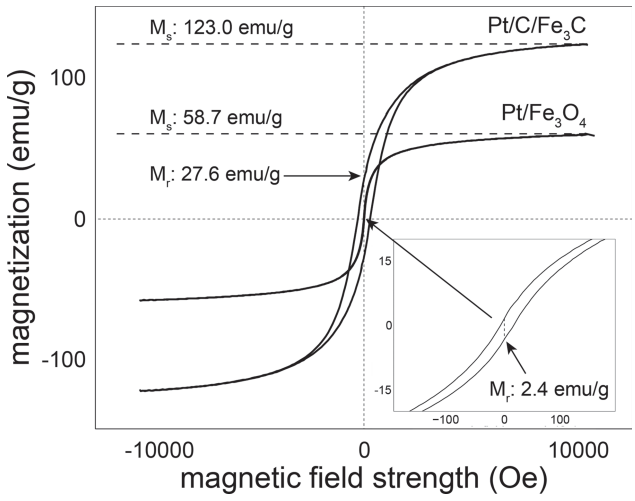

Figure 3. Vibrating sample magnetometry hysteresis curves of platinum-spiked cementite (Pt/C/Fe_3C) and magnetite (Pt/Fe_3O_4) particles. The almost superparamagnetic magnetite particles show a substantially lower saturation magnetization than the cementite particles.

thicknesses of 1–2 nm. This well-structured and very thin coating ensures high chemical resistivity[18] of the core material and furthermore allows a chemical functionalization by forming stable carbon-carbon bonds to the graphene-like surface.[13] The magnetite nanoparticles in Figure 2c appear as close to spherical crystallites with a size distribution between 5 and 25 nm. Corresponding X-ray diffractograms (Figure 2b,d) confirm a cementite, respectively magnetite phase. Due to the low platinum content of both particle types, indications for larger platinum crystals, if present, would be hardly observable in the diffraction patterns. Ideally, a platinum doping within the magnetite and the cementite crystal lattice occurs, which is not visible in XRD. As TEM images did not show any separate crystallites (high contrast) which can be addressed to platinum and the harsh pretreatment of Pt/C/Fe_3C with 24% HCl did not result in any shift of the platinum concentration due to different dissolution characteristics (verified by ICP-MS measurements), it can be concluded that platinum is well-dispersed within both materials and not present as a separate phase.

Vibrating sample magnetometry was used to determine both the saturation magnetization and the magnetic remanence of the materials. The cementite particles reveal a significantly higher saturation magnetization (123.0 emu g^{-1}) compared to the magnetite particles (58.7 emu g^{-1}). The remanence of the cementite particles was found to be 27.6 emu g^{-1}, whereas the magnetite particles revealed an (almost) superparamagnetic behavior (remanence 2.4 emu g^{-1}) as shown in **Figure 3**. The magnetic characteristics changed only slightly after the chemical modification with PEG groups as the functional loading only accounts for around 3 wt% of the material according to elemental microanalysis in **Table 1**.

Table 1. C, H, N contents of the different materials determined by elemental microanalysis as well as platinum contents determined using ICP-MS.

Material	C [wt%]	H [wt%]	N [wt%]	Pt [wt%]
Pt/Fe_3O_4	2.01	0.53	0.07	0.090 ± 0.001
Pt/C/Fe_3C	9.87	0.04	0.01	0.105 ± 0.001
PEG-Pt/Fe_3O_4	3.46	0.75	0.18	0.088 ± 0.001
PEG-Pt/C/Fe_3C	13.04	0.24	0.14	0.101 ± 0.001

Magnetic first order reversal curve (FORC) analysis is able to identify different magnetic phases which are present in a sample and therefore, in contrast to vibrating sample magnetometry (VSM), not only provides averaged information about the magnetic properties of a sample. Interactions between magnetic domains as well as size effects become apparent with this technique. The obtained FORC diagrams depicted in **Figure 4**a,b reveal a single phase for both materials (i.e., absence of multiple spots), which is in good agreement with the obtained XRD diffractograms. Furthermore, both profiles are almost narrow and almost symmetric in H_U direction (distribution of interaction fields), which suggests that

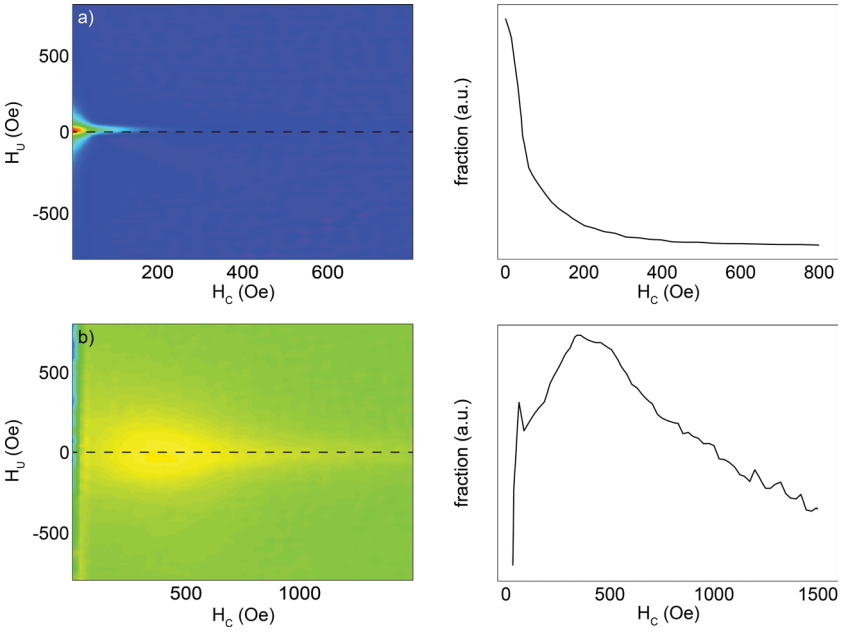

Figure 4. a) FORC diagram of Pt/Fe_3O_4 revealing a single magnetic phase with magnetically independent domains (i.e., symmetrical in H_U direction). b) FORC diagram of Pt/C/Fe_3C showing magnetically independent domains. c) Centered coercivity distribution of Pt/Fe_3O_4 revealing a large fraction of superparamagnetic particles and a smaller fraction of particles (larger) with a magnetic coercivity. d) Centered coercivity distribution of Pt/C/Fe_3C. The material shows a broad coercivity distribution compared to the magnetite material, superparamagnetic particles are absent.

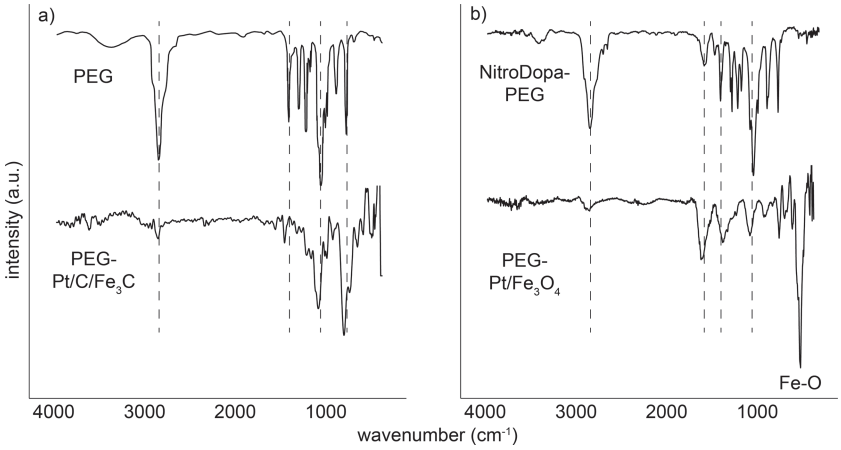

Figure 5. Diffuse reflectance infrared Fourier transform spectra (DRIFTS) of the chemically functionalized cementite a) and magnetite b) nanomagnets and structure confirmation by comparison to the pure surfactant compounds. Peak shifts and intensity changes are a result of binding to the surface and changes in molecular symmetry. The magnetite particles show a Fe-O stretching vibration at around 560 cm^{-1}.

the particles appear as magnetically independent domains. The centered coercivity plot of Pt/Fe_3O_4 in Figure 4c reveals that a large fraction of the magnetite nanomagnets shows a superparamagnetic behavior, whereas a smaller particle fraction (larger in size) is responsible for the residual magnetic remanence of the material which was quantified by VSM. The centered coercivity plot of $Pt/C/Fe_3C$ in Figure 4d shows a broad coercivity profile and superparamagnetic particles are absent.

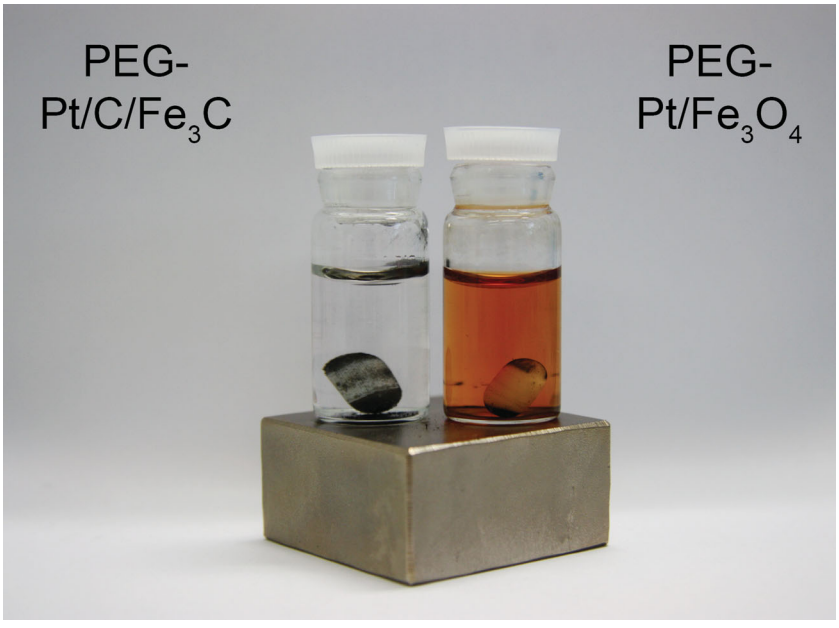

Figure 6. Magnetically separated PEG-$Pt/C/Fe_3C$ (left) and PEG-Pt/Fe_3O_4 (right) in 0.1 M HCl after 1 h of vigorous stirring. The presence of potassium thiocyanate in the supernatant leads to the formation of an orange complex when ionic iron is present in the solution. The magnetite based material shows a strong leaching compared to the cementite based material.

3.2. Surface Functionalization

PEG surface functionalizations are well-known to enhance the biocompatibility of nanomagnets in a major extent[21] and furthermore strongly enhance their aqueous dispersibility.[16] The PEG surface functionalization of both materials was confirmed by DRIFTS as shown in **Figure 5**. The obtained spectra were compared to the spectra of the corresponding pure surfactants and show a good agreement. Moreover, a strong stretching vibration absorption band at around 560 cm^{-1}, characteristic for magnetite,[22] can be observed.

3.3 Particle Degradation and Leaching

Measuring the nanoparticle concentration in a biological media is not straight forward and is hindered by the complexity of the matrix. In addition, potential particle disintegration, generally labeled as leaching could lead to misinterpretations concerning the remaining particle amount in biological samples as dissolved material will not be magnetically removed, but would be considered as remaining particles in a sample from an analytical point of view. Therefore, knowledge about the particle stability is pivotal for a reliable quantification in biological samples. Iron-oxide based magnetic nanomaterials are considerably less stable against dissolution than carbon-coated metal nanomagnets.[23] Thus, it must be clarified whether leaching could occur under the examined conditions and time frames. Small amounts of material were stirred in PBS and in a second experimental run in 0.1 M HCl as explained in the experimental section (to simulate chemically harsh, but biologically irrelevant conditions). The iron-concentration in the PBS solutions remained below the limit of detection after 1 h (approx. 0.2 mg kg^{-1} iron or 0.06 wt% particle loss), which is a typical duration for a proposed magnetic dialysis[24]. Under the relatively harsh acidic conditions (0.1 M HCl) 1.90 wt% of PEG-Pt/Fe_3O_4 dissolved, whereas only 0.14 wt% of PEG-$Pt/C/Fe_3C$ disintegrated. The significantly higher leaching of the magnetite based material is illustrated in **Figure 6**, where the iron release into the surrounding medium is visualized by the formation of the orange thiocyanate complex. These results clearly highlight the significantly higher chemical stability of the carbon-coated nanomagnets and the eligibility of the here applied protocols to quantify particles by platinum spiking under physiological conditions.

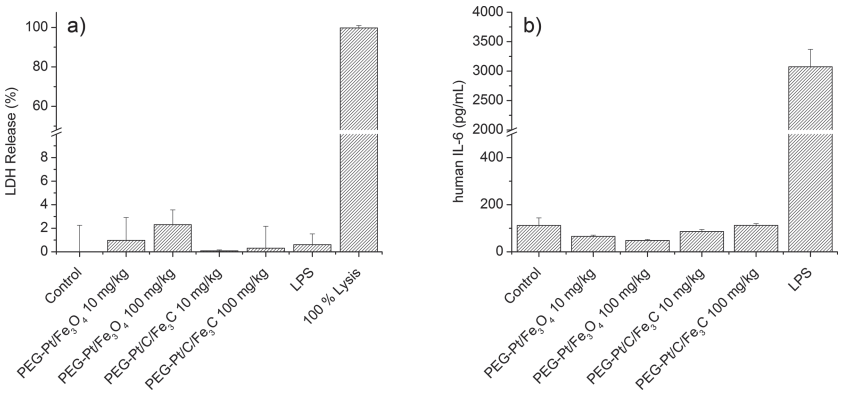

Figure 7. a) LDH release of human microvascular endothelial cells which were exposed to polyethylene coated magnetite and cementite particles. There are no significant differences in protein release compared to the control. b) h-IL6 concentrations in the cell media after 20 h of incubation showing no increased inflammatory responses compared to the control.

3.4. Platinum Quantification in the Nanomagnets (and in Blood Samples)

By quantification with ICP-MS the platinum concentrations of the PEG-functionalized nanomagnets were determined. For this purpose several blank blood samples were spiked with small amounts of particles. The results listed in Table 1 confirm a good agreement between the added amount of platinum in the precursor solution and the concentration found in the particles.

3.5. Cytocompatibility of Platinum-Doped Nanomagnets

The surface functionalization of particles is the key parameter for biocompatibility. Polyethyleneglycol coatings are known as good dispersion agents and are frequently used to enhance the biological compatibility.[16] Cytocompatibility of the synthesized nanoparticles was measured by exposing human microvascular endothelial cells, which line the blood vessels, to nanoparticles for a time period of 20 h. The release of lactate dehydrogenase (LDH, a protein which is released upon break down of the cellular membrane) was then quantified as a measure for cytotoxicity. Human interleukin 6 (hIL-6) was quantified as a measure for potential inflammatory reactions in response to particles exposure. There were no significant differences in the h-IL6 concentration as well as LDH release for the different particle types and concentrations compared to the controls after 20 h of incubation (**Figure 7**). Therefore it can be concluded that the nanomagnets do not reveal any obvious adverse effects on the used tissue cultures under the examined conditions.

3.5.1. Nanoparticle Detection in Biosamples by Means of Platinum Content Measurements

Blood, on average, contains around close to 0.9 wt% (i.e., 9000 mg kg^{-1}) dissolved salts.[25] ICP-MS used for trace element analysis is sensitive to high salt loadings. After the digestion procedure the samples were diluted in two subsequent steps to obtain an acceptable salt load of around 100 mg kg^{-1} (1:1000). Therefore, an initial concentration of 1 mg particles with 0.1 wt% platinum per mL of blood results in a platinum content of around 1 µg kg^{-1} after dilution. The limit of detection in the here used protocols was in the range of 5 ng kg^{-1} platinum, or 5 mg kg^{-1} particles in blood respectively. The quantification of even lower platinum concentrations with mass spectrometry is cumbersome and therefore discloses the limits of the here used quantification technique. Higher platinum doping of the particles to enhance (lower) the detection capabilities could alter the material properties in a considerable extent and moreover leads to platinum phase segregation (i.e., no doping any more). This could lead to misinterpretations of the particle concentration after a magnetic separation as platinum crystals could not be properly conjoined to the nanomagnets.

3.6. Magnetic Separation from Human Whole Blood

3.6.1. Stationary Extraction Experiments

Unlike to dispersions in pure water the magnetic separation occurs comparatively rapid in ion-rich buffers or blood. The effectiveness of stabilizing agents such as polyethylene glycols is limited in media with high salt concentrations. Thus, particles can aggregate easier, which strongly influences the magnetic separation velocity enhancement factor.[8] These effects manifest in the results of the stationary separation experiments depicted in **Figure 8** where a particle contaminated blood volume of 1 mL was cleaned. In a rapid initial extraction phase within

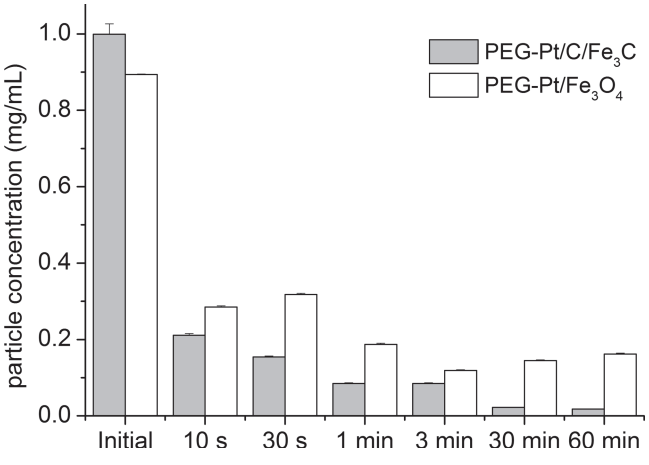

Figure 8. Remaining magnetic particle concentrations in blood samples after stationary magnetic extraction. After a rapid initial separation period, the progress is slowed down as the proximity to the magnet is not sufficient at all sections of the vial. In contrast to the cementite particles, the magnetite particles which were too distant from the magnet could not be collected even after prolonged exposition to the magnetic field.

Table 2. Nanomagnet separation efficiency under different flow conditions

Material	Low flow [2.4 mm s^{-1}]	High flow [30 mm s^{-1}]
PEG-Pt/Fe_3O_4	>99.5%	56.0%
PEG-Pt/C/Fe_3C	>99.5%	>99.5%

the first seconds the concentrations of both particle types were strongly depressed, whereas the separation of the cementite particles occurred slightly more rapidly. Thereafter, the cementite concentration further decreased, whereas the magnetite concentration got only slightly lower and finally stagnated. The used vials for the separation had a diameter of 28 mm. A close proximity to the strong magnet becomes critical for a complete and rapid separation. A higher saturation magnetization of the extracted particles not only enhances their separation rate, but also the separation reach within a stagnant medium.

3.6.2. In-Flow Extraction Experiments

Different flow velocities within various blood vessels are going along with different shear stress levels. A higher blood flow velocity therefore increasingly complicates a reliable and efficient nanomagnet separation by an external magnetic field. In a first in-flow separation experiment a moderate blood flow velocity (2.4 mm s^{-1}) was chosen. This flow is comparable to the flow conditions that can be found in small venules (<20 μm inner diameter), whereas a higher flow (30 mm s^{-1}) was chosen to simulate the flow in a larger, therapeutically relevant vein (<5 mm inner diameter).[26] **Table 2** shows the relative particle concentration levels of both PEGylated magnetic nanomaterials in contaminated human blood before and after a simple magnetic separator under low- and high-flow conditions. In the low-flow scenario both materials were separated to such an extent, that the platinum content of the blood samples was below the limit of detection. Under high-flow conditions however, only 56% of the magnetite material was removed, whereas the cementite level in the samples still remained below the limit of detection. In this context, it must be highlighted that the here used magnetite particles still reveal a high saturation magnetization after their chemical functionalization with PEG surface groups (around 3 wt% carbon increase for both materials following elemental microanalysis results in Table 1). In most reported works[14,27] PEGylated magnetite particles, mostly due to high functional loadings, reveal significantly lower saturation magnetizations (a few emu g^{-1}). The separation performance of these materials suffers strongly when being extracted from biological samples, resulting in prolonged separation durations and incomplete separation. Under flow-conditions, where the residence time at the separation point is usually system-inherently limited, this can result in serious disadvantages of such kinds of materials.

4. Conclusion

The viscosity of biological fluids makes rapid movement of magnetic particles challenging. A high magnetization is required to provide sufficient force for targeted particle movement, particularly in a flow situation. Disadvantageous agglomeration effects can be suppressed by chemical modification (e.g., PEG[24]). This study shows that the commonly cited necessity for superparamagnetic behavior in magnetic particles is of limited validity.[28] While the chemical stability of carbon-encapsulated metal nanoparticles offers significant technological advantages, it may have its downside in terms of safety when applied in vivo, and biomedical treatments will have to account for the fate of traces of particles that remain in a patient for a prolonged time. The here proposed platinum doping allows quantitative analysis of tissue sections or blood when using iron-based nanoparticles, even though biological background iron as well as salt concentrations are high (matrix effects). The capability to reliably remove magnetic nanoparticles from flowing blood now permits development of magnetic blood extraction, where a noxious compound is mechanically removed out of a living organism.

Acknowledgements

We thank Dr. Frank Krumeich for the transmission electron microscopy imaging and Mr. Hanspeter Hächler for the vibrating sample magnetometry. Financial support by ETH Zurich, the Swiss National Science Foundation (No. 406440-131268 and 206021-133768) and the Forschungskredit of the University of Zurich (No. 54345802) is kindly acknowledged.

Received: February 25, 2013
Published online: April 17, 2013

[1] a) Q. A. Pankhurst, N. T. K. Thanh, S. K. Jones, J. Dobson, *J. Phys. D: Appl. Phys.* **2009**, *42*, 224001; b) A. K. Gupta, M. Gupta, *Biomaterials* **2005**, *26*, 3995; c) Q. A. Pankhurst, J. Connolly, S. K. Jones, J. Dobson, *J. Phys. D: Appl. Phys.* **2003**, *36*, R167; d) V. Wagner, A. Dullaart, A. K. Bock, A. Zweck, *Nat. Biotechnol.* **2006**, *24*, 1211.

[2] a) S. Kayal, R. V. Ramanujan, *Mater. Sci. Eng., C* **2010**, *30*, 484; b) S. J. Guo, D. Li, L. M. Zhang, J. Li, E. K. Wang, *Biomaterials* **2009**, *30*, 1881; c) A. Amirfazli, *Nat. Nanotechnol.* **2007**, *2*, 467; d) D. A. LaVan, T. McGuire, R. Langer, *Nat. Biotechnol.* **2003**, *21*, 1184.

[3] a) B. Basly, D. Felder-Flesch, P. Perriat, C. Billotey, J. Taleb, G. Pourroy, S. Begin-Colin, *Chem. Commun.* **2010**, *46*, 985; b) H. B. Na, I. C. Song, T. Hyeon, *Adv. Mater.* **2009**, *21*, 2133; c) M. Uchida, M. Terashima, C. H. Cunningham, Y. Suzuki, D. A. Willits, A. F. Willis, P. C. Yang, P. S. Tsao, M. V. McConnell, M. J. Young, T. Douglas, *Magn. Reson. Med.* **2008**, *60*, 1073; d) R. Y. Hong, B. Feng, L. L. Chen, G. H. Liu, H. Z. Li, Y. Zheng, D. G. Wei, *Biochem. Eng. J.* **2008**, *42*, 290; e) M. Zhao, D. A. Beauregard, L. Loizou, B. Davletov, K. M. Brindle, *Nat. Med.* **2001**, *7*, 1241.

[4] a) M. Mahmoudi, S. Sant, B. Wang, S. Laurent, T. Sen, *Adv. Drug Delivery Rev.* **2011**, *63*, 24; b) Z. X. Li, M. Kawashita, N. Araki, M. Mitsumori, M. Hiraoka, M. Doi, *Mater. Sci. Eng. C* **2010**, *30*, 990; c) E. Andronescu, M. Ficai, G. Voicu, D. Ficai, M. Maganu, A. Ficai, *J. Mater. Sci.* **2010**, *21*, 2237; d) S. Mohapatra, S. K. Mallick, T. K. Maiti, S. K. Ghosh, P. Pramanik, *Nanotechnology* **2007**, *18*; e) Z. L. Cheng, A. Al Zaki, J. Z. Hui, V. R. Muzykantov, A. Tsourkas, *Science* **2012**, *338*, 903.

[5] C. X. Fan, W. H. Gao, Z. X. Chen, H. Y. Fan, M. Y. Lie, F. J. Deng, Z. L. Chen, *Int. J. Pharm.* **2011**, *404*, 180.

[6] a) M. Zhang, D. Cheng, X. W. He, L. X. Chen, Y. K. Zhang, *Chem.-Asian J.* **2010**, *5*, 1332; b) M. Takahashi, T. Yoshino, H. Takeyama, T. Matsunaga, *Biotechnol. Prog.* **2009**, *25*, 219; c) S. Mandal, A. Ghosh, M. Mandal, *Prep. Biochem. Biotechnol.* **2009**, *39*,

20; d) J. Jin, F. Yang, F. W. Zhang, W. Q. Hu, S. B. Sun, J. T. Ma, *Nanoscale* **2012**, *4*, 733.
[7] I. K. Herrmann, M. Urner, F. M. Koehler, M. Hasler, B. Roth-Z'Graggen, R. N. Grass, U. Ziegler, B. Beck-Schimmer, W. J. Stark, *Small* **2010**, *6*, 1388.
[8] I. K. Herrmann, R. N. Grass, W. J. Stark, *Nanomedicine* **2009**, *4*, 787.
[9] V. Schaller, U. Kraling, C. Rusu, K. Petersson, J. Wipenmyr, A. Krozer, G. Wahnstrom, A. Sanz-Velasco, P. Enoksson, C. Johansson, *J. Appl. Phys.* **2008**, *104*, 093918.
[10] C. Heneghan, D. Langton, M. Thompson, *Br. Med. J.* **2012**, *344*, e1349.
[11] a) S. H. Sun, H. Zeng, *J. Am. Chem. Soc.* **2002**, *124*, 8204; P. A. Dresco, V. S. Zaitsev, R. J. Gambino, B. Chu, *Langmuir* **1999**, *15*, 1945; b) W. W. Yu, J. C. Falkner, C. T. Yavuz, V. L. Colvin, *Chem. Commun.* **2004**, *20*,2306; c) Z. H. Zhou, J. Wang, X. Liu, H. S. O. Chan, *J. Mater. Chem.* **2001**, *11*, 1704; d) Y. L. Hou, J. F. Yu, S. Gao, *J. Mater. Chem.* **2003**, *13*, 1983.
[12] I. K. Herrmann, R. N. Grass, D. Mazunin, W. J. Stark, *Chem. Mater.* **2009**, *21*, 3275.
[13] R. N. Grass, E. K. Athanassiou, W. J. Stark, *Angew. Chem. Int. Ed.* **2007**, *46*, 4909.
[14] E. Amstad, M. Textor, E. Reimhult, *Nanoscale* **2011**, *3*, 2819.
[15] J. Xie, C. Xu, N. Kohler, Y. Hou, S. Sun, *Adv. Mater.* **2007**, *19*, 3163.
[16] E. Amstad, T. Gillich, I. Bilecka, M. Textor, E. Reimhult, *Nano Lett.* **2009**, *9*, 4042.
[17] S. B. Bubenhofer, C. M. Schumacher, F. M. Koehler, N. A. Luechinger, R. N. Grass, W. J. Stark, *J. Phys. Chem. C* **2012**, *116*, 16264.
[18] C. M. Schumacher, R. N. Grass, M. Rossier, E. K. Athanassiou, W. J. Stark, *Langmuir* **2012**, *28*, 4565.
[19] G. T. Hermanson, *Bioconjugate Techniques*, Academic Press, WalthamMA, USA **2008**, 707.
[20] I. K. Herrmann, M. Urner, M. Hasler, B. Roth-Z'Graggen, C. Aemisegger, W. Baulig, E. K. Athanassiou, S. Regenass, W. J. Stark, B. Beck-Schimmer, *Nanomedicine* **2011**, *6*, 1199.
[21] J. Sun, S. B. Zhou, P. Hou, Y. Yang, J. Weng, X. H. Li, M. Y. Li, *J. Biomed. Mater. Res., Part A* **2007**, *80A*, 333.
[22] F. Marquez, G. M. Herrera, T. Campo, M. Cotto, J. Duconge, J. M. Sanz, E. Elizalde, O. Perales, C. Morant, *Nanoscale Res. Lett.* **2012**, *7*, 210.
[23] A. Schaetz, M. Zeltner, T. D. Michl, M. Rossier, R. Fuhrer, W. J. Stark, *Chem.-Eur. J.* **2011**, *17*, 10565.
[24] I. K. Herrmann, R. E. Bernabei, M. Urner, R. N. Grass, B. Beck-Schimmer, W. J. Stark, *Nephrol. Dial. Transplant.* **2011**, *26*, 2948.
[25] A. M. Butler, E. M. MacKay, *J. Biol. Chem.* **1934**, *106*, 107.
[26] R. Klinke, C. Bauer, *Physiologie*, *Vol. 5*, Thieme, Stuttgart **2005**, p. 174.
[27] a) J. Y. Park, P. Daksha, G. H. Lee, S. Woo, Y. M. Chang, *Nanotechnology* **2008**, *19*, 365603; b) A. Shkilnyy, E. Munnier, K. Herve, M. Souce, R. Benoit, S. Cohen-Jonathan, P. Limelette, M. L. Saboungi, P. Dubois, I. Chourpa, *J. Phys. Chem. C* **2010**, *114*, 5850.
[28] M. Zeltner, R. N. Grass, A. Schaetz, S. B. Bubenhofer, N. A. Luechinger, W. J. Stark, *J. Mater. Chem.* **2012**, *22*, 12064.